



HHS Public Access

Author manuscript

ACS Nano. Author manuscript; available in PMC 2015 June 23.

Published in final edited form as:

ACS Nano. 2008 August ; 2(8): 1696–1702. doi:10.1021/nn800275r.

Self-Assembled Lipid-Polymer Hybrid Nanoparticles: A Robust Drug Delivery Platform

Liangfang Zhang¹, Juliana M Chan², Frank X Gu¹, June-Wha Rhee³, Andrew Z Wang^{1,3}, Aleksandar F Radovic-Moreno¹, Frank Alexis^{1,3}, Robert Langer¹, and Omid C Farokhzad^{3,*}

¹Department of Chemical Engineering and Division of Health Science and Technology, Massachusetts Institute of Technology, Cambridge, MA 02139

²Department of Biology, Massachusetts Institute of Technology, Cambridge, MA 02139

³Laboratory of Nanomedicine and Biomaterials, Department of Anesthesiology, Brigham Women's Hospital, Harvard Medical School, Boston, MA 02115

Abstract

We report the engineering of a novel lipid-polymer hybrid nanoparticle (NP) as a robust drug delivery platform, with high drug encapsulation yield, tunable and sustained drug release profile, excellent serum stability, and potential for differential targeting of cells or tissues. The NP is comprised of three distinct functional components: i) a hydrophobic polymeric core where poorly water-soluble drugs can be encapsulated; ii) a hydrophilic polymeric shell with anti-biofouling properties to enhance NP stability and systemic circulation half-life; and iii) a lipid monolayer at the interface of the core and the shell that acts as a molecular fence to promote drug retention inside the polymeric core, thereby enhancing drug encapsulation efficiency, increasing drug loading yield, and controlling drug release. The NP is prepared by self-assembly through a single-step nanoprecipitation method in a reproducible and predictable manner, making it potentially suitable for scale-up

Keywords

polymeric nanoparticles; liposome; self-assembly; nanoprecipitation; drug delivery

Introduction

Nanotechnology has been exploited extensively to enhance the pharmacokinetic properties and therapeutic index of a myriad of drugs^{1–4}. In the past two decades, a large number of nanoparticle-based therapeutic products have entered clinical development or been approved for clinical use⁵. Polymeric nanoparticles (NPs) and liposomes represent two dominant classes of nanocarriers capable of efficiently encapsulating and delivering a variety of drug classes^{5, 6}. Polymeric NPs which are suitable for systemic administration may be formed by self-assembly of biodegradable copolymers consisting of two or more polymer blocks with different hydrophobicities. The use of amphiphilic polymers results in formation of NPs

*Corresponding authors: ofarokhzad@zeus.bwh.harvard.edu.

with a hydrophobic core and a hydrophilic shell. The core-shell structure of polymeric NPs allows them to: encapsulate and carry poorly water-soluble drugs; decrease the biofouling of the NPs resulting in long circulation half-life; release drugs at a sustained rate in the optimal range of drug concentration; and be further functionalized with targeting ligands for differential delivery⁷⁻⁹. In addition, the preparation of polymeric NPs based on the nanoprecipitation or double emulsion methods is simple and scalable⁷. For example, Genexol-PM is a NP formulation of paclitaxel and poly (*D,L*-lactide)-*b*-polyethylene glycol-methoxy, which has been approved for metastatic breast cancer therapy in Korea¹⁰. Liposomes are spherical lipid vesicles with a bilayer structure of natural or synthetic amphiphilic lipid molecules. Liposomes have been widely used as drug delivery vehicles because of favorable safety profile, ease of surface modification, and long systemic circulation half-life that can reach days after being surface modified with hydrophilic polymers such as polyethylene glycol (PEG)^{11, 12}. Several liposomal drug formulations have been approved for clinical use including Doxil (doxorubicin liposomes)¹³ which was first to be approved in 1995, AmBisome (amphotericin B liposomes), DaunoXome (daunorubicin liposomes), DepoCyt (cytarabine liposomes), DepoDur (morphine liposomes), and Visudyne (verteporfin liposomes)^{5, 12}.

Given the clinical success of polymeric NPs and liposomes, we hypothesized that a lipid-polymer hybrid NP may be developed that takes advantage of the unique strengths of polymeric NPs and liposomes. The hybrid NPs can be a robust drug delivery platform with high drug encapsulation yield, tunable and sustained drug release profile, excellent serum stability, and potential for differential targeting of cells or tissues. Previously polymeric NPs were mixed with liposomes to form lipid-polymer complexes such as lipoparticles where the lipid bilayer or lipid multi-layer fuses on the surface of polymeric NPs¹⁴⁻¹⁶. These complexes usually require a two-step formulation process: i) development of polymeric NPs, and ii) encapsulation of polymeric NPs within liposomes, resulting in a poor control over the final NP physicochemical structure which may hinder their clinical translation. It is desirable to develop lipid-polymer hybrid NPs using a well-defined and predictable formulation strategy in a single-step, which may facilitate future scale up.

Here we report a platform to engineer sub-100 nm targeted lipid-polymer hybrid NPs through a combination of nanoprecipitation and self-assembly. These NPs combine the desirable characteristics of polymer NPs and liposomes, while excluding some of their intrinsic limitations. The NPs are comprised of three distinct functional components: i) a biodegradable hydrophobic polymeric core that can carry poorly water-soluble bioactive drugs and release them at a sustained rate; ii) a stealth material forming a hydrophilic shell that can allow the particles to evade recognition by immune system components and increase particle systemic circulation half life; and iii) a lipid monolayer at the interface of the hydrophobic core and the hydrophilic shell, which can prevent the carried agents from freely diffusing out of the NPs and reduce water penetration rate into the NPs, thereby enhancing drug encapsulation yield and slowing drug release from the NPs. For targeted delivery purposes, the surface of NPs can be functionalized with targeting molecules that can bind to unique molecular signatures on cells or tissues of interest.

Results and Discussion

In this study, we used ester terminated poly _{D,L}-lactic-co-glycolic acid (PLGA) as a model hydrophobic polymer to form the polymeric core of the NPs; polyethylene glycol (PEG), which is covalently conjugated to 1,2-distearoyl-sn-glycero-3-phosphoethanolamine (DSPE), as a model hydrophilic polymer to form the “stealth” shell of the NPs; and lecithin as a model lipid to form the lipid monolayer at the interface of PLGA core and PEG shell. Since both PLGA and DSPE-PEG polymers have been approved by the Food and Drug Administration (FDA) for medical applications and lecithin is a natural lipid extracted from soybean, we expect the lipid-polymer hybrid NPs should be biocompatible, biodegradable, and potentially safe as a drug carrier for clinical use. As illustrated in Figure 1A, the lipid-polymer hybrid NPs are self-assembled from PLGA, lecithin and DSPE-PEG conjugate through a single-step nanoprecipitation method. Specifically, PLGA polymer precipitates to form a hydrophobic core to encapsulate poorly water soluble drugs. Lecithin and DSPE-PEG conjugate self-assemble around the PLGA core to form a lipid monolayer covered by a PEG shell. To characterize the structure of the NPs, they were imaged by transmission electron microscopy (TEM) with negative staining by uranyl acetate which stains lecithin and the lipids conjugated with PEG to enhance their electron density resulting in a dim ring surrounding the PLGA core (Figure 1B). The thickness of the ring is less than 5 nm which equals the thickness of a lecithin monolayer plus a PEG shell. The lipid / polymer weight ratio and PLGA molecular weight may be changed to fine tune NP size (diameter, nm) and surface charge (zeta potential, mV), to achieve the optimal NP pharmacokinetic properties *in vivo*. As shown in Figure 1C, the lipid / polymer weight ratio of 10~20% results in NPs with favorable combination of size (70~80 nm) and zeta potential (−30~−35 mV) for drug delivery application¹⁷. One possible explanation is that at this ratio, the amount of lipids is in the range to cover the entire surface of the PLGA hydrophobic core. However, when the ratio of lipid to polymer is too high, the excess lipids may increase above the critical micellar concentration (CMC) of lecithin (~0.4 mg/mL, data from manufacturer) resulting in the assembly of lecithin liposomes (typical size is about 100~1000 nm). The coexistence of these liposomes would enhance the overall measured size of the hybrid NPs and lower their zeta potential value. Conversely, when the lipid / polymer weight ratio is too low, there is a paucity of lipids to cover the surface of the PLGA core resulting in a high zeta potential value (close to bare PLGA NPs). In the following studies, we formulated lipid-polymer hybrid NPs (1 mg/mL) using a lipid / polymer weight ratio of 10% translating to a starting lipid concentration of 0.1 mg/mL, which is lower than the CMC of lecithin. Dynamic light scattering measurements further demonstrated that liposomes are not formed at the low concentration of lecithin used in our protocol. By keeping the lipid / polymer weight ratio constant at 10% we varied the PLGA inherent viscosity and demonstrated that we can fine tune NP size in a highly reproducible manner while minimally affecting NP surface charge. For example, when the inherent viscosity of PLGA was increased from 0.19 to 0.82, the NP size dropped from 92.7±2.0 nm (Polydispersity=0.211±0.008, Mean±SD, N=3) to 66.7±4.5 nm (Polydispersity=0.244±0.0048, Mean±SD, N=3) (Figure 1D) while the NP zeta potential only slightly fluctuated in the range of −30.2~−34.3 mV. The observed effect of polymer inherent viscosity on NP size was quite consistent with what has been previously reported for PLGA-PEG polymeric NPs¹⁸. A possible mechanism is that higher molecular weight

polymers precipitate to form more compact structures during the process of nanoprecipitation as compared to equivalent polymers with a lower molecular weight.

Next we examined drug encapsulation yield, loading yield and release profile of the lipid-polymer hybrid NPs in comparison with PLGA-PEG polymeric NPs and PLGA polymeric NPs. We hypothesized that the addition of a lipid monolayer at the interface of the PLGA core and the PEG shell may serve two distinct functions: i) to prevent small drug molecules from freely diffusing out of the PLGA core, thereby improving drug encapsulation yield and loading yield, and ii) to reduce the water penetration rate into the PLGA core thereby decreasing the rate of hydrolysis of PLGA polymers resulting in slower drug release from the NPs. To test these hypotheses, docetaxel (Dtxl), a widely used anticancer drug, was selected as a model hydrophobic drug to be encapsulated in the lipid-polymer hybrid NPs. As shown in Figure 2A, when Dtxl was mixed with PLGA at the weight ratio of 5 to 100 and dissolved in acetonitrile for the preparation of lipid-polymer hybrid NPs, 59±4% (Mean ±SD, N=3) of Dtxl was encapsulated into the NPs. In contrast, Dtxl encapsulation yields of PLGA-PEG NPs and PLGA NPs were approximately 19±3% (Mean±SD, N=3) and 37±4% (Mean±SD, N=3), respectively. The relatively low encapsulation yield of PLGA-PEG NPs may stem from the possibility that some PEG blocks were buried inside PLGA-PEG diblock copolymer NPs during nanoprecipitation process which results in a less hydrophobic core than the pure PLGA polymeric core of both the lipid-polymer hybrid NPs and the PLGA NPs. In addition, the encapsulated Dtxl was released from the hybrid NPs at a sustained rate over 120 hours (Figure 2B). When lipid-polymer hybrid NPs, PLGA-PEG NPs, and PLGA NPs were each loaded with Dtxl at approximately 3 wt%, it took the hybrid NPs around 20 hrs to release 50% of Dtxl vs. 10 hrs and 7 hrs for PLGA-PEG NPs and PLGA NPs, respectively. These results indicate that the lipid monolayer at the interface of the PLGA core and the PEG shell acts as a molecular fence that helps to retain the drugs inside the NPs. We further observed that the high Dtxl encapsulation yield and the sustained drug release characteristics of these hybrid NPs are retained across a broad range of Dtxl input during NP formulation. For example, when the initial Dtxl input was 5%, 10% and 15% of the weight of the PLGA polymer, the measured loading yield reached 3.0%, 6.1% and 8.5% respectively, which corresponded to a nearly constant encapsulation yield of 60% (Figure 2C). However, Dtxl encapsulation yield dropped when the initial drug input was increased to 20%. We also found that Dtxl was released from the hybrid NPs at a sustained manner until its loading yield was higher than ~6% (Figure 2D).

NP stability in serum is an important criterion for their utility as drug carriers *in vivo*. Using the change in NP size in the presence of plasma as a surrogate for protein adsorption and biofouling, we next studied the serum stability of lipid-polymer hybrid NPs. We incubated the lipid-polymer hybrid NPs with 10% bovine serum albumin (BSA) solution and 10% human plasma solution and monitored changes in NP size over time. As controls, PLGA-PEG polymeric NPs and PLGA polymeric NPs were similarly tested in parallel. As shown in Figure 3 A and B, the hybrid NPs and the PLGA-PEG NPs were stable in 10% BSA solution retaining their size of 90±2 nm (Polydispersity=0.223±0.011, Mean±SD, N=3), while a slight increase in size was observed in 10% plasma solution. In contrast, PLGA NPs had a dramatic size increase from 90 nm to 200~300 nm within 10 minutes of incubation in

BSA or plasma. Consistent with previous reports we observed that the presence of PEG prevented protein adsorption on NP surface, and the resulting decrease in NP biofouling has previously been shown to prolong NP systemic circulation half-life.

We next demonstrated the suitability of these lipid-polymer hybrid NPs for targeted delivery applications. To this end, we covalently conjugated amine terminated A10 RNA aptamers to carboxyl functionalized lipid-PEG conjugates using 1-ethyl-3-(3-dimethylaminopropyl) carbodiimide (EDC) and N-hydroxysuccinimide (NHS) activation chemistry, and used these lipid-PEG-aptamer conjugates in the self-assembly of lipid-polymer hybrid NPs. The A10 aptamer is a nuclease-stabilized 2'-fluoropyrimidine RNA molecule with 57 base pairs which has shown high binding affinity to the prostate specific membrane antigen (PSMA) overexpressed by some prostate cancer (PCa) cell lines¹⁹. In the study, LNCaP prostate adenocarcinomas, which express the PSMA antigen on their plasma membrane, were chosen as the target cell line for *in vitro* testing; PC3 prostate adenocarcinomas, which do not express the PSMA antigen, were employed as a negative control. To visualize cell uptake of the NPs using fluorescence microscopy, a hydrophobic fluorescent probe, NBD-cholesterol (22-(N-(7-nitrobenz-2-oxa-1,3-diazol-4-yl)amino)-23,24-bisnor-5-cholesterol-3 β -ol) (Excitation/Emission=460nm/534nm), was encapsulated inside the hybrid NPs²⁰. Figure 4 showed that PSMA-targeted NBD-encapsulated hybrid NPs were differentially taken up by LNCaP cells which express the PSMA protein (Figure 4A) but not PC3 cells which do not express the PSMA protein (Figure 4C). The small amount of NBD signal from PC3 cells may represent a portion of free NBD released from the NPs during the incubation time or alternatively may represent non-specific uptake of particles by the PC3 cells. When PSMA aptamer was not used, negligible amount of non-targeted NPs were delivered to LNCaP (Figure 4B) and PC3 (Figure 4D) cells. A recent report from our laboratory demonstrated the advantages of forming targeted NPs in a single-step process using a mixture of PLGA-PEG diblock copolymers and preformed PLGA-PEG-Aptamer triblock copolymers¹⁸. In contrast to the conventional two-step process that PLGA-PEG NPs were first prepared and then surface functionalized with aptamer, this single-step synthesis approach allows one to produce large-scale targeted NPs while minimizing production time and NP batch-to-batch variation. However, problems arise when generalizing this idea to protein-based targeting systems using antibodies or affibodies simply because proteins can not tolerate the harsh reaction environment with PLGA-PEG polymer in organic solvent. Speculatively, the lipid-polymer hybrid NPs presented in this paper may provide a way to solve this problem. One can conjugate protein-based targeting ligands with lipid-PEG in an aqueous environment to form a lipid-PEG-ligand triblock structure and then mix it with lipid-PEG and other components to form a targeted lipid-polymer hybrid NP in a single-step nanoprecipitation process.

Conclusion

In summary, we have developed a lipid-polymer hybrid NP platform consisting of a hydrophobic polymeric core, a hydrophilic polymeric shell and a lipid monolayer at the interface of the core and the shell. These lipid-polymer hybrid NPs combine the merits of the polymeric NPs and liposomes. It has been demonstrated that the hybrid NP has tunable size and surface charge, high drug loading yield, sustained drug release profile, favorable stability in serum, good cellular targeting ability and its simple synthesis process may be

amenable to further scale-up if desired. All these positive attributes make the lipid-polymer hybrid NPs a promising drug delivery vehicle for further *in vivo* evaluation.

Methods

NP preparation

Lipid-polymer hybrid NPs were prepared via self-assembly of PLGA (poly (D,L-lactic-co-glycolic acid); Lactel, Pelham, AL), lecithin (soybean, refined, molecular weight: ~330 Da; Alfa Aesar, Ward Hill, MA), and DSPE-PEG (1,2-distearoyl-sn-glycero-3-phosphoethanolamine- N-carboxy (polyethylene glycol)2000); Avanti, Alabaster, AL) through a single-step nanoprecipitation method. Briefly, PLGA polymer was dissolved in acetonitrile with concentrations ranging from 1~5 mg/mL. Lecithin/DSPE-PEG (8.5/1.5, molar ratio) with a weight ratio of 15% to the PLGA polymer were dissolved in 4 wt% ethanol aqueous solution. The lecithin/DSPE-PEG solution was heated to 65°C to ensure all lipids were in liquid phase. The resulting PLGA solution was then added into the preheated lipid solution dropwise under gentle stirring. The mixed solution was vortexed vigorously for 3 minutes followed by gentle stirring for 2 hours at room temperature. The remaining organic solvent and free molecules were removed by washing the NP solution three times using an Amicon Ultra-4 centrifugal filter (Millipore, Billerica, MA) with a molecular weight cut-off of 10,000 Da. To prepare drug-encapsulated NPs, docetaxel (Sigma-Aldrich, St Louis, MO) with proper initial dosage was dissolved into the PLGA acetonitrile solution before the nanoprecipitation process. NP size (diameter, nm) and surface charge (zeta potential, mV) were obtained from three repeat measurements by Quasi-elastic laser light scattering with a ZetaPALS dynamic light scattering detector (15 mW laser, incident beam = 676 nm; Brookhaven Instruments Corporation, Holtsville, NY).

Drug loading and release study

To measure the drug loading yield and release profile of docetaxel (Dtxl) from each type of NPs, 3 mL NP PBS solutions at a concentration of 5 mg/mL were split equally into 30 Slide-A-Lyzer MINI dialysis microtube with a molecular weight cut-off of 3,500 Da (Pierce, Rockford, IL). These microtubes were dialyzed in 4 L PBS buffer at 37 °C with gentle stirring. PBS buffer was changed every 24 hours during the whole dialysis process. At each data point, NP solutions from three microtubes were collected separately and mixed with an equal volume of acetonitrile to dissolve the NPs. The resulting free Dtxl content in each microtube was assayed using an Agilent (Palo Alto, CA) 1100 HPLC equipped with a pentafluorophenyl column (Curosil-PFP, 250 ×4.6 mm, 5μ; Phenomenex, Torrance, CA). Dtxl absorbance was measured by a UV-vis detector at 227 nm and a retention time of 12 minutes in 1 mL/min 50/50 acetonitrile/water mobile phase.

NP *in vitro* stability

NPs were incubated with 10 wt% BSA (bovine serum albumin; Sigma-Aldrich, St Louis, MO) solution and 10 wt% human plasma (BioChemMed, Winchester, VA) solutions respectively at 37 °C under gentle stirring at a concentration of 1 mg/mL. At each time point, an aliquot of NP solutions was collected to measure NP size using Quasi-elastic laser light scattering. The measurements were performed in triplicate at room temperature.

Fluorescence microscopy

To visualize cellular uptake of aptamer-targeted lipid-polymer hybrid NPs using fluorescence microscopy, a hydrophobic fluorescent dye, NBD-cholesterol (22-(N-(7-nitrobenz-2-oxa-1,3-diazol-4-yl)amino)-23,24-bisnor-5-cholen-3 β -ol; Invitrogen, Carlsbad, CA), was encapsulated inside the NPs. The fluorescence emission spectrum of NBD (Excitation/Emission = 460nm/534nm) was detected in the green channel (490nm/528nm) of a Delta Vision RT Deconvolution Microscope. In the study, the prostate LNCaP and PC3 cell lines were grown in 8-well microscope chamber slides in RPMI-1640 and Ham's F-12K medium respectively, both supplemented with 100 units/ml aqueous penicillin G, 100 μ g/mL streptomycin, and 10% FBS (fetal bovine serum) at concentrations to allow 70% confluence in 24 hours (i.e., 40,000 cells per cm²). On the day of experiments, cells were washed with pre-warmed PBS buffer and incubated with pre-warmed fresh media for 30 minutes before adding NPs with a final concentration of ~ 250 μ g/mL (N=4). Cells were incubated with the NPs for 2 hours at 37 $^{\circ}$ C, washed two times with PBS (300 μ L per well), fixed with 4% formaldehyde, and mounted with non-fluorescent mounting medium DAPI (Cector Laboratory, Inc. Burlingame, CA). The cells were then imaged using a Delta Vision RT Deconvolution Microscope.

Acknowledgement

We thank Philip Kantoff and Neil Bander for helpful discussions throughout this study. This work was supported by National Institutes of Health Grants CA119349 and EB003647 and David Koch-Prostate Cancer Foundation Award in Nanotherapeutics. J.M.C. acknowledges the financial support from the Agency for Science, Technology and Research, Singapore.

References

1. Ferrari M. Cancer Nanotechnology: Opportunities and Challenges. *Nat. Rev. Cancer.* 2005; 5:161–171. [PubMed: 15738981]
2. Langer R. Drug Delivery and Targeting. *Nature.* 1998; 392:5–10. [PubMed: 9579855]
3. Jiang W, Kim BYS, Rutka JT, Chan WCW. Nanoparticle-Mediated Cellular Response is Size-Dependent. *Nat. Nanotechnol.* 2008; 3:145–150. [PubMed: 18654486]
4. Farokhzad OC, Langer R. Nanomedicine: Developing Smarter Therapeutic and Diagnostic Modalities. *Adv. Drug. Deliv. Rev.* 2006; 58:1456–1459. [PubMed: 17070960]
5. Zhang L, Gu FX, Chan JM, Wang AZ, Langer RS, Farokhzad OC. Nanoparticles in Medicine: Therapeutic Applications and Developments. *Clin. Pharmacol. Ther.* 2008; 83:761–769. [PubMed: 17957183]
6. Wagner V, Dullaart A, Bock AK, Zweck A. The Emerging Nanomedicine Landscape. *Nat. Biotechnol.* 2006; 24:1211–1217. [PubMed: 17033654]
7. Farokhzad OC, Cheng J, Teply BA, Sherifi I, Jon S, Kantoff PW, Richie JP, Langer R. Targeted Nanoparticle-Aptamer Bioconjugates for Cancer Chemotherapy *in vivo*. *Proc. Natl. Acad. Sci. U S A.* 2006; 103:6315–6320. [PubMed: 16606824]
8. Torchilin VP. Micellar Nanocarriers: Pharmaceutical Perspectives. *Pharm. Res.* 2007; 24:1–16. [PubMed: 17109211]
9. Tong R, Cheng JJ. Anticancer Polymeric Nanomedicines. *Polymer Reviews.* 2007; 47:345–381.
10. Kim TY, Kim DW, Chung JY, Shin SG, Kim SC, Heo DS, Kim NK, Bang YJ. Phase I and Pharmacokinetic Study of Genexol-PM, a Cremophor-Free, Polymeric Micelle-Formulated Paclitaxel, in Patients with Advanced Malignancies. *Clin. Cancer Res.* 2004; 10:3708–3716. [PubMed: 15173077]

11. Moghimi SM, Szebeni J. Stealth Liposomes and Long Circulating Nanoparticles: Critical Issues in Pharmacokinetics, Opsonization and Protein-Binding Properties. *Prog. Lipid Res.* 2003; 42:463–478. [PubMed: 14559067]
12. Torchilin VP. Recent Advances with Liposomes as Pharmaceutical Carriers. *Nat. Rev. Drug Discov.* 2005; 4:145–160. [PubMed: 15688077]
13. Skubitz KM. Phase II Trial of Pegylated-Liposomal Doxorubicin (Doxil) in Sarcoma. *Cancer Invest.* 2003; 21:167–176. [PubMed: 12743981]
14. De Miguel I, Imbertie L, Rieumajou V, Major M, Kravtsoff R, Betbeder D. Proofs of the Structure of Lipid Coated Nanoparticles (SMBV) Used as Drug Carriers. *Pharm. Res.* 2000; 17:817–824. [PubMed: 10990200]
15. Wong HL, Bendayan R, Rauth AM, Wu XY. Simultaneous Delivery of Doxorubicin and GG918 (Elacridar) by New Polymer-Lipid Hybrid Nanoparticles (PLN) for Enhanced Treatment of Multidrug-Resistant Breast Cancer. *J. Control. Release.* 2006; 116:275–284. [PubMed: 17097178]
16. Thevenot J, Troutier AL, David L, Delair T, Ladaviere C. Steric Stabilization of Lipid/Polymer Particle Assemblies by Poly(ethylene glycol)-Lipids. *Biomacromolecules.* 2007; 8:3651–3660. [PubMed: 17958441]
17. Moghimi SM, Hunter AC, Murray JC. Long-Circulating and Target-Specific Nanoparticles: Theory to Practice. *Pharmacol. Rev.* 2001; 53:283–318. [PubMed: 11356986]
18. Gu F, Zhang L, Teply BA, Mann N, Wang A, Radovic-Moreno AF, Langer R, Farokhzad OC. Precise Engineering of Targeted Nanoparticles by Using Self-Assembled Biointegrated Block Copolymers. *Proc. Natl. Acad. Sci. U S A.* 2008; 105:2586–2591. [PubMed: 18272481]
19. Lupold SE, Hicke BJ, Lin Y, Coffey DS. Identification and Characterization of Nuclease-Stabilized RNA Molecules That Bind Human Prostate Cancer Cells *via* the Prostate-Specific Membrane Antigen. *Cancer Res.* 2002; 62:4029–4033. [PubMed: 12124337]
20. Zhang L, Radovic-Moreno AF, Alexis F, Gu FX, Basto PA, Bagalkot V, Jon S, Langer RS, Farokhzad OC. Co-Delivery of Hydrophobic and Hydrophilic Drugs from Nanoparticle-Aptamer Bioconjugates. *ChemMedChem.* 2007; 2:1268–1271. [PubMed: 17600796]

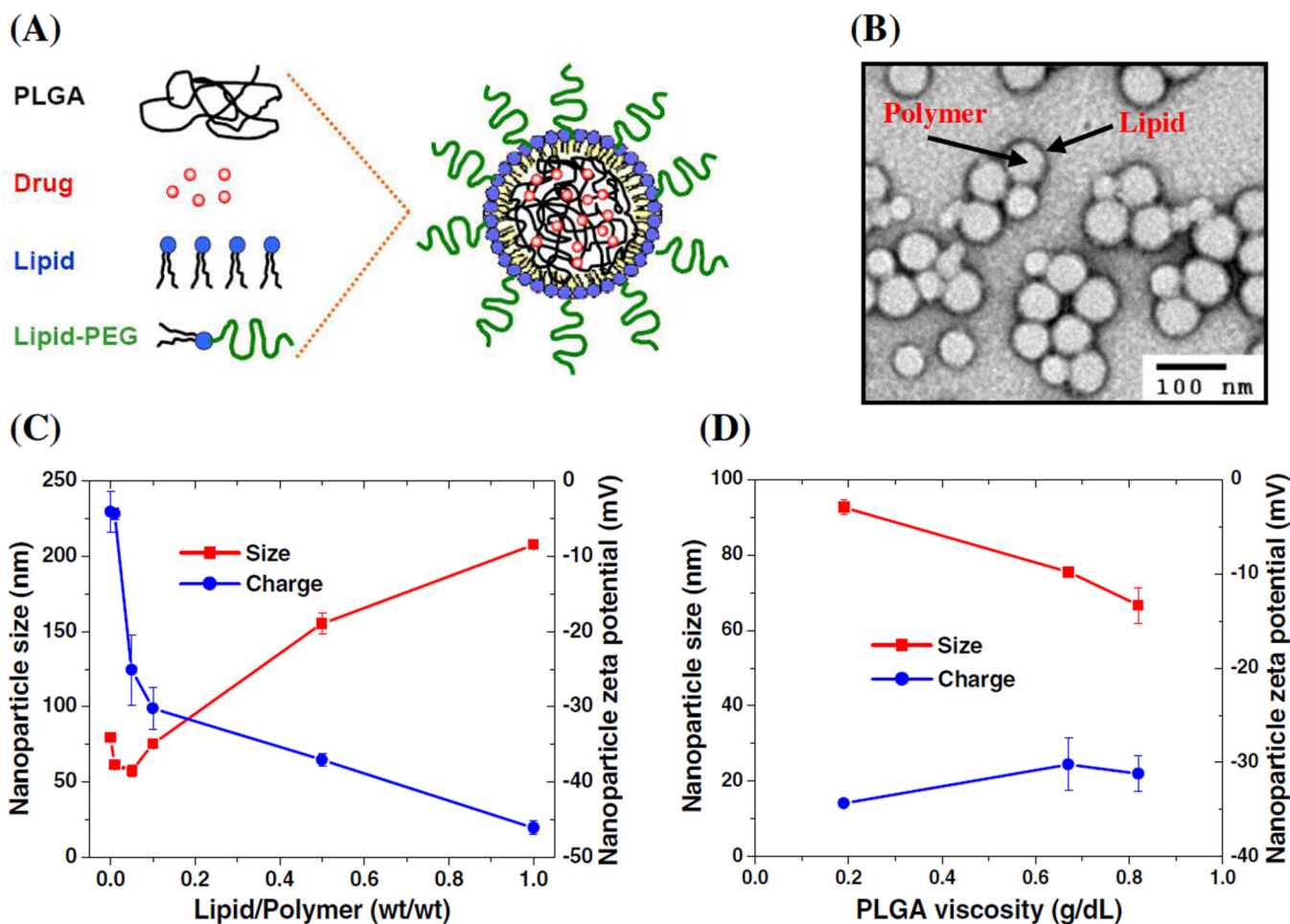


Figure 1.

Development of lipid-polymer hybrid nanoparticles (NPs). **(A)** A schematic illustration shows the formulation of lipid-polymer hybrid NPs. The NPs are comprised of a hydrophobic PLGA (poly lactic-co-glycolic acid) core, a hydrophilic PEG (polyethylene glycol) shell, and a lipid (lecithin) monolayer at the interface of the hydrophobic core and the hydrophilic shell. **(B)** Transmission electron microscopy (TEM) image demonstrated the structure of the hybrid NPs proposed in (A). Uranyl acetate was used to stain lipids to enhance their electron contrast. **(C)** Effect of lipid/polymer weight ratio on NP size and surface zeta potential. **(D)** Effect of PLGA polymer molecular weight indicated as inherent viscosity on NP size and surface zeta potential.

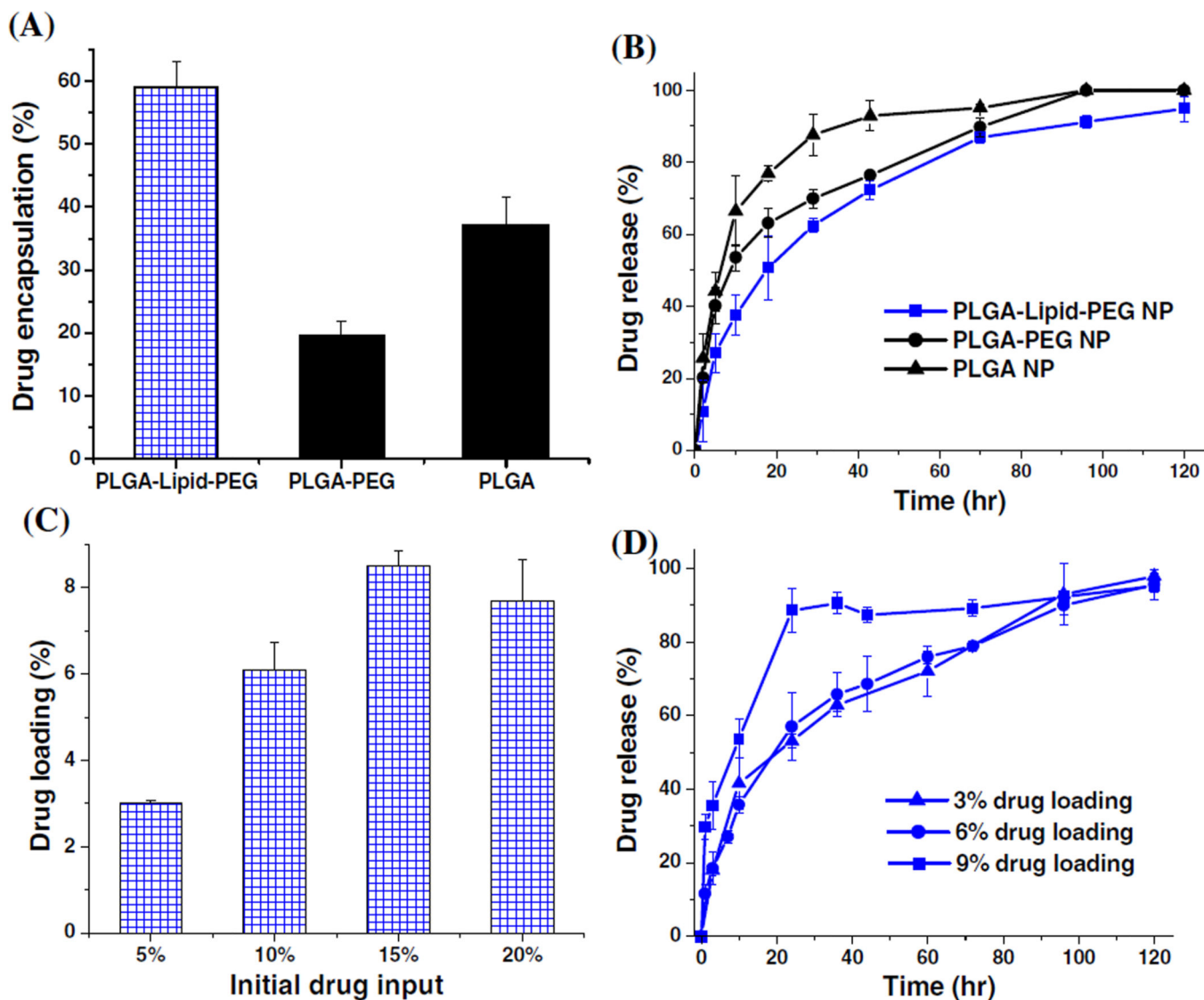


Figure 2. Drug carrying capacity and release profile of lipid-polymer hybrid NPs. Docetaxel (a widely used anticancer drug) was used as a model small molecule hydrophobic drug. **(A)** Drug encapsulation yield of PLGA-Lipid-PEG hybrid NPs in comparison with PLGA-PEG polymeric NPs and PLGA polymeric NPs. Total initial drug input was 5 wt% of the weight of PLGA polymer for each type of NPs. **(B)** Drug release profiles from PLGA-Lipid-PEG NPs, PLGA-PEG NPs and PLGA NPs respectively. Drug loading was 3 wt% for each type of NPs. **(C)** Drug loading yield of PLGA-Lipid-PEG NPs at various initial drug inputs ranging from 5 wt% to 20 wt% of the weight of PLGA polymer. **(D)** Drug release profiles from PLGA-Lipid-PEG NPs with a drug loading of 3 wt%, 6 wt% and 9 wt% respectively.

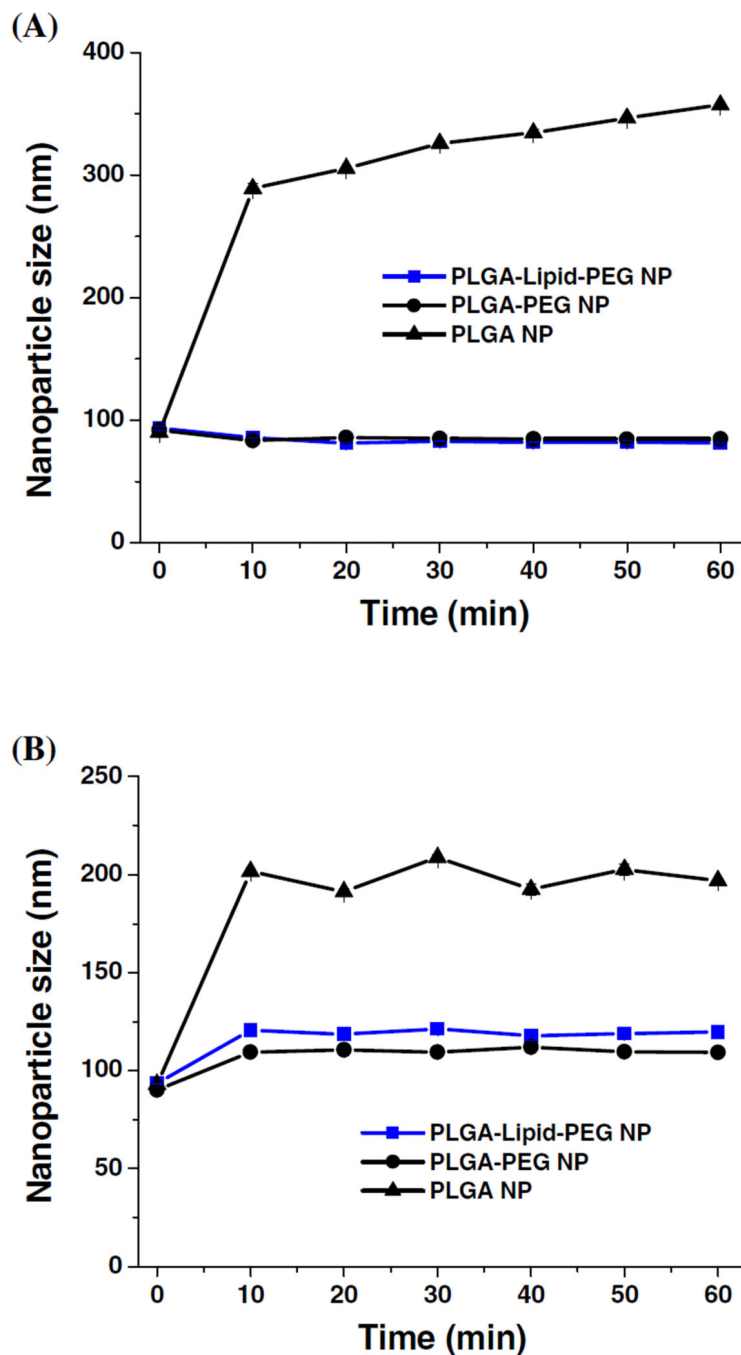


Figure 3. NP size temporal stability *in vitro*. PLGA-Lipid-PEG hybrid NPs (blue squares), PLGA-PEG NPs (black circles) and PLGA NPs (black triangles) were incubated with (A) 10 wt% BSA (Bovine Serum Albumin) solution, and (B) 10 wt% plasma with heparin solution respectively at 37 °C under gentle stirring. At each time point, an aliquot of NP suspensions was removed to measure NP size using ZetaPALS dynamic light-scattering.

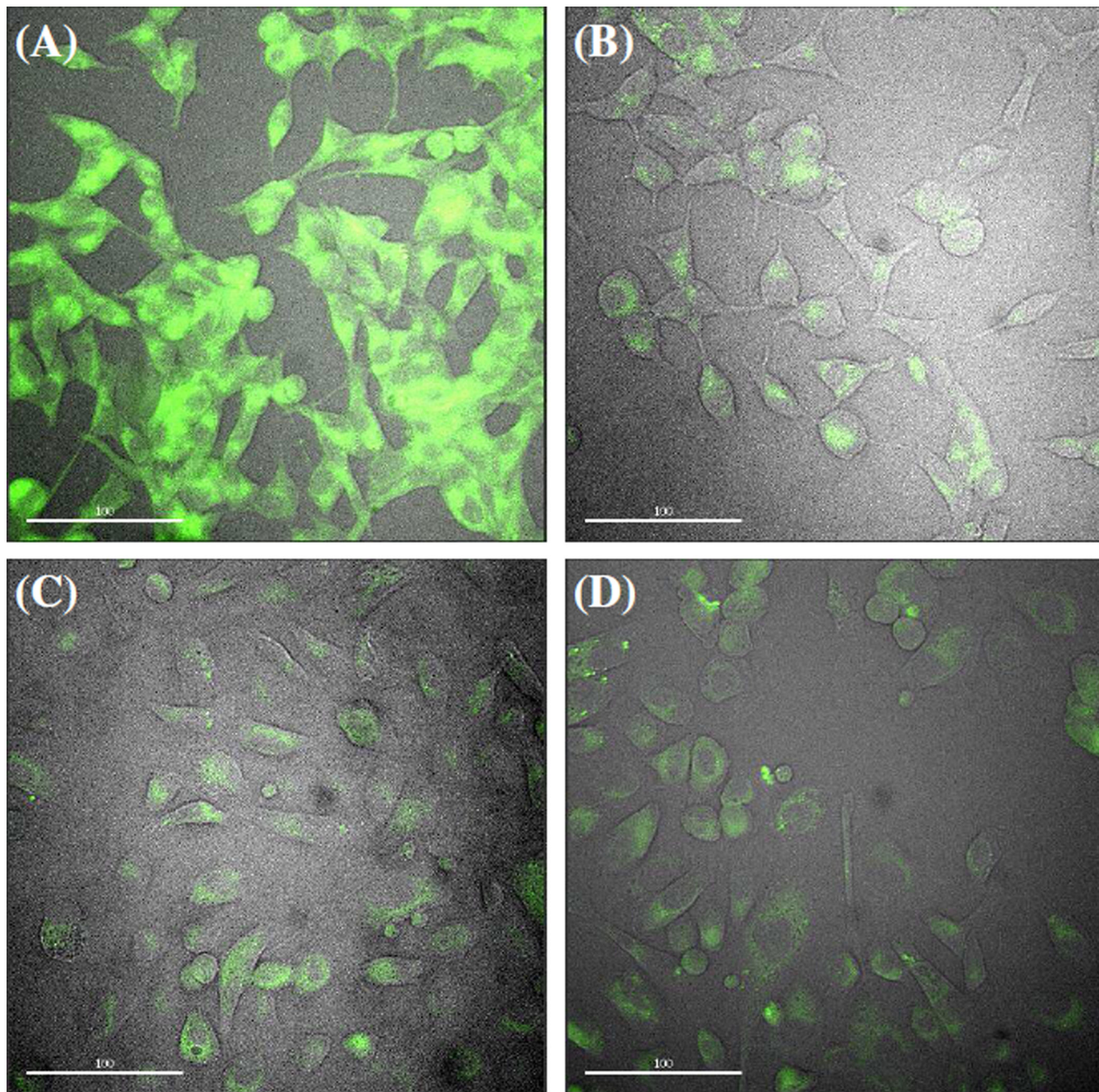


Figure 4. Binding sensitivity and specificity of lipid-polymer hybrid NPs surface modified with A10 RNA aptamer. The aptamer specifically binds to prostate specific membrane antigen (PSMA) which is overexpressed by prostate epithelial cells. For imaging, hydrophobic fluorescence dye NBD (green) was encapsulated inside the NPs. Fluorescence scanning microscopy images demonstrated that aptamer-targeted NPs were selectively delivered to LNCaP cells which overexpress PSMA protein (A) but not PC3 cells which do not express

PSMA protein (**C**), and non-targeted NPs did not preferentially bind to either LNCaP (+PSMA) cells (**B**) or PC3 (-PSMA) cells (**D**). The scale bar in all images is 100 μm .

Author Manuscript

Author Manuscript

Author Manuscript

Author Manuscript